Title: A low-cost test rig for impact experiments on a dummy head

Authors: Ahmad Yaser Alhaddad(a,b), John-John Cabibihan(a), Ahmad Hayek(a), and Andrea Bonarini(b)

Affiliations: a) Qatar University, Department of Mechanical and Industrial Engineering, Doha 2713, Qatar. b) Politecnico di Milano, Department of Electronics, Information and Bioengineering, Piazza Leonardo da Vinci 32, Milano 20133, Italy.

Contact email: john.cabibihan@qu.edu.qa

Abstract: Anthropomorphic test dummies are commonly used to evaluate the potential harm to humans due to dangerous scenarios (e.g. car accidents). Furthermore, they have been used in sports to study the potential harm to the head (e.g. concussions) due to impacts. In this article, we describe the development of a low-cost dummy head experimental setup. The motivation behind this project is to quantify the potential harm to a child's head due to impacts with a small robotic toy. Three severity indices can be estimated, namely, Head Acceleration Criterion (HIC), 3 ms criterion, and peak head acceleration. 3D-printed parts were used to develop the head. A tri-axial accelerometer embedded inside the head was used to measure the changes in accelerations. The developed head was placed inside a dedicated experimental bench. A data acquisition card was used to acquire the raw data while a computer system was used to store and then provide the analysis. The developed experimental setup was validated by producing comparable results to that of relevant previous studies.

Keywords: Head safety, Severity indices, Children safety, Small robots, Test rig

Specifications table:

Hardware name	Head impact test rig
Subject area	- Mechanical Engineering - Safety Engineering
Hardware type	- Mechanical engineering - Field measurements and sensors
Open source license	Creative Commons (CC) BY 4.0
Cost of hardware	$ 900 - $ 3795 (with DAQ cost)
Source file repository	https://data.mendeley.com/datasets/wsxphrmydn/1

1. Hardware in context

Anthropomorphic test dummies (ATDs) are used to evaluate the potential harm to humans through the simulation of risky scenarios, for example, using ATD in car crash tests. Such dummies are equipped with sensors to measure different dynamics that occur due to impacts, such as accelerations and forces. Severity indices are used to assess the potential for an injury based on the measured dynamics. For example, the acceleration of the head due to impact is used to compute the Head Injury Criterion (HIC) numerical value, which in turn is used to predict the potential for harm based on the Abbreviated Injury Scale (AIS) [1].

The application of test dummies has been also considered in other areas, such as in sports. For the assessment of protective gears in sports, ATDs based setups were used [2][3]. The evaluation was based on simulating impacts that might occur in actual scenarios. In a study evaluating concussion due to taekwondo kicks, a dummy head was used to measure the dynamics of the head due to impacts [4]. In that study, a 50th percentile ATD head (i.e. Hybrid II) with a mass of 5.1 kg attached to a neck was used. The internal structure of the head was made of aluminum covered with an artificial skin layer while the neck was made of rubber. The head setup was fitted with a taekwondo head guard that was then mounted on an aluminum support frame. A tri-axial accelerometer was embedded at the center of the head to obtain the linear acceleration of the head. The readings of the accelerometer was acquired through a three-channel sensor signal conditioner connected to a computer. A motion analysis system consisting of eight cameras was used to monitor the head's movement and to measure the peak velocity of the kicks through tracking reflective markers placed on the test head and the foot pads. The participants were requested to perform different kicks on the dummy head while wearing the foot pads.

Furthermore, such setups were also considered to assess harm in robotics by considering different scenarios where a robot is impacting a person at different body parts [5][6]. Alternative approaches, such as low-cost sensors and body parts models, were also considered to conduct impact experiments [7][8].One study considered a low-cost developed head model to conduct impact experiments to characterize a safety index in robotics [9]. In that study, the impacts were performed by robotic arm (i.e. Scara Robot-Adept Cobra 600) at different impact speed conditions (i.e. 0.4 - 1.9 m/s). The developed head model was based on a leather ball filled with sand to reach a weight of 3 kg. A low-cost tri-axial accelerometer was placed at the head to measure the linear acceleration of the head. Furthermore, that study has considered a low-cost sensor to measure the impact force placed at the point of impact.

In this work, we present a low-cost method for the construction of a dummy head experimental setup to conduct impact experiments at low velocities. The impact rig is focused on investigating impacts due to thrown objects. The developed rig does not require expensive hardware (e.g. expensive camera system) and can be constructed using typical available facilities (e.g. 3D printer). Some suggested equipment can be substituted by cheaper alternatives.

2. Severity indices

2.1 Head Injury Criterion

One of the most commonly used severity index to measure the possible injury to the head in many applications, such as automotive and sports [10], and it is defined as:

$$HIC = (t_2 - t_1) \left[\frac{1}{(t_2 - t_1)} \int_{t_1}^{t_2} a(t) \, dt \right]^{2.5} \tag{1}$$

Table 1: Classification of tissue injury based on depth [20]

Classification	Affected Skin Layer	Depth
Superficial	Only the epidermis	<1 mm
Partial-thickness	The epidermis and into the dermis	1 - 4 mm
Full-thickness	Through the epidermis and the dermis into subcutaneous tissue	>4 mm
Subcutaneous	Extends into and beyond the subcutaneous tissue	>4 mm

where $a(t)$ is based on the resultant acceleration of the head and measured in terms of gravity acceleration ($g = 9.81\frac{m}{s^2}$) and $\Delta t = t_2 - t_1$ is the duration of the impact considered in calculating the resultant HIC. 36 ms and 15 ms are the two most commonly used durations to evaluate the severity of injury to the head with the 15 ms being more restrictive. The developed rig considers the 36 ms in the HIC evaluation.

2.2 3 ms Criterion

This criterion demands that the maximum average over 3 ms duration of the resultant head acceleration to be less than a certain threshold when there is no hard contact. The European National Car Assessment Protocol (EnuroNCAP) states that the thresholds for 3 ms criterion for a child occupant should not exceed 87 g in case of frontal impact and 72 g in case of side impact [11].

2.3 Peak Linear Acceleration

The peak linear acceleration of the head has been used as one of the biomechanical measures to investigate concussion due to impacts [12],[13]. The reported range of the linear accelerations due to impacts in youth football is 10 to 111 g [14]. Within that range, concussion events could occur based on the reported incidents [15]. One study used a validated FEM head model to estimate the probability of a mild TBI [16]. That study has shown that there is a 25% chance of a concussion occurrence corresponding to a head's acceleration of 66 g. Finally, concussion could occur at an acceleration as low as 31.8 g as reported by another study [17].

2.4 Tissue Injuries

The impact rig uses an artificial skin that can be used as an indicator for tissue injuries. Damage to the skin due to impacts with objects take on various forms. For example, impacts could cause abrasions, skin tears, and lacerations. The shape of the impactor and the pressure force involved influence the depth of the injury and its magnitude [19]. The depth of an injury is often to classify wounds and tissue injuries [20]. Based on the depth, tissue injuries can be classified to either superficial wounds, partial-thickness, full-thickness or subcutaneous skin loss (Table. 1). We suggest using this classification as an indicator to investigate the potential for tissue injuries due to impacts in this rig.

3. Hardware description

The experimental setup is a device to examine the acceleration changes of the head due to impacts. It reports the head acceleration in the X, Y, and Z directions. The setup is suitable for the examination of low velocity impacts. The setup would be beneficial for researchers who have limited access to more expensive test dummies. The analysis of the acceleration data can report three severity indices. Modifications are possible to perform different forms of impact tests. The setup offers the following:

- Reporting of the head accelerations (i.e. in X, Y, and Z axes) and the resultant acceleration

- Post processing of the raw data provides the analysis for three severity indices

- Adjustable to do different tests at different impact velocities

- The dummy head mass can be modified to meet different age groups

- The rig is adjustable to perform different tests (e.g. different impact areas)

- The artificial skin of the dummy head can be used as an indicator for tissue injuries

4. Design files

This section contains a summary to the design files that have been used to build the impact rig. All files can be found in their respective links in the online repository.

4.1 Design Files Summary

Design file name	File type	Description	Open source license	Location of the file
human-head-part1	STL file	The modified front half of the original head design (Fig. 1b)	CC BY 4.0	Link 1
human-head-part2	STL file	The modified back half of the original head design (Fig. 1c)	CC BY 4.0	Link 2
Exp_bench	PDF	A reference drawing of the experimental bench that was used showing the dimensions.	CC BY 4.0	Link 3
labview_script	National instruments VI file	A script that reads the accelerometer that is connected to the data acquisition card and stores the readings.	CC BY 4.0	Link 4
Matlab_script_multi	MATLAB code	A code to calculate the three severity indices, namely, the HIC, 3 ms, and peak acceleration.	CC BY 4.0	Link 5

5. Bill of materials

This section contains the complete bill of materials that were used to construct the impact rig.

Designator	Component	Number	Cost per unit currency (US$)	Total cost(US$)	Source of materials	Material type
ACC	ADXL 377	1	$ 25.95	$ 25.95	SparkFun Electronics	Electronics
DAQ	PCI-6031E[1]	1	$ 2,895.00	$ 2,895.00	National Instrument	Electronics
Camera	FDR-X1000V[2]	1	$ 500.00	$ 500.00	Sony	Electronics
Tripod	Amazon Basics 50-Inch Lightweight Tripod	1	$ 15.00	$ 15.00	Amazon	Aluminum
Wires	Ribbon Cable -6 wires 15ft	2	$ 2.95	$ 5.90	SparkFun Electronics	Cables
3D printing material	PLA Material Large Spool[3]	2	$ 48	$ 96	MakerBot Industries	Polylactic acid
Soft material	Ecoflex 00-30 (2 lbs)	1	$ 32.21	$ 64.42	Smooth-On	Silicone rubber
Mass	Modeling clay	2	~$ 10	~$ 20	Amazon or Local stores	Polymer clay
Frame	Custom-made experimental setup bench	1	~$ 150	~$ 150	Local mechanical workshop	Stainless steel
Rope	Coated ropes	1	$ 5	$ 5	Local stores	Nylon
Velcro	Velcro Elastic Straps (36" x 1")	2	~$ 7	~$ 14	Amazon or local stores	Nylon, Polyester
PVC	Plastic Saddle Elbow (1")	2	$ 2	$ 4	Local stores	Plastic

---

[1]Alternative DAQ can be considered as long as it provides a high sampling rate (e.g. 20 kHz).

[2]Alternative video camera can be used that can record in slow-motion at high frame rates (i.e. equal or greater than 200 fps).

[3]Filament purchased should be compatible with the 3D printer available.
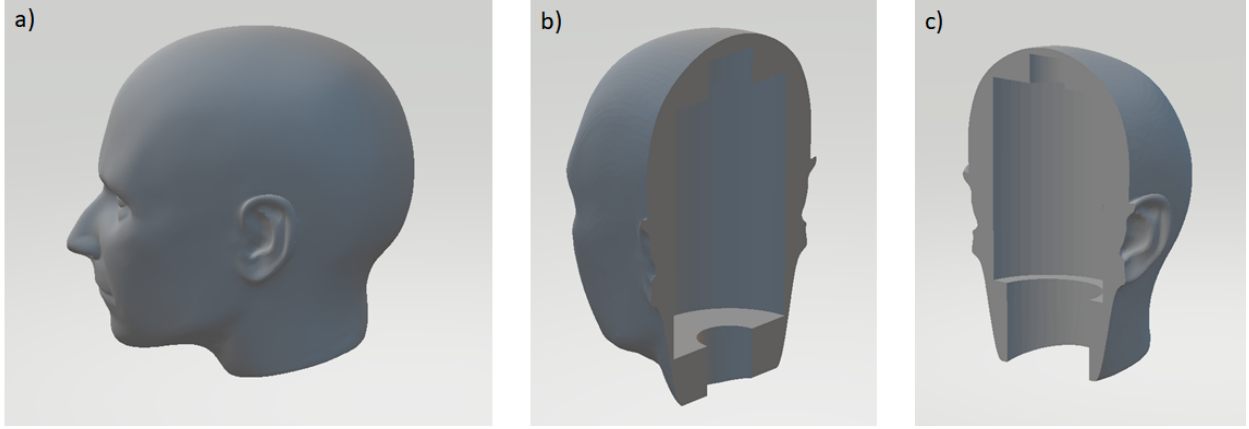
Figure 1: The 3D head design that was used to develop the dummy head. a) Complete view of the original design (Source: Link). b) Part 1 view (i.e. front). c) Part 2 view (i.e. back).

6. Build instructions

6.1 Experimental setup

The two files of the head design (i.e. human-head-part1 and human-head-part2) were developed by a 3D printer (Replicator 5th Generation, MakerBot Industries). The settings of the 3D printer were left at default. The infill option was set at 10%. If more robustness or higher mass is required, then this option should be set at higher percentages. However, this will increase the time required to print the parts considerably. Soft materials can be added to make the skin more lifelike [21][22][23][24][25]. Hence, a 2 mm layer of a soft material made of silicone was added to the head [26]. The soft material (Ecoflex, Smooth-On, USA) was prepared by mixing equal volume (i.e. 1A:1B) of the two material parts for around 4 mins. The soft material was then applied to both parts of the head then left to cure for 4 hours at room temperature (Fig. 2). Other soft materials can also be considered (e.g. PDMS [27]). Furthermore, embedding other sensors (e.g. pressure or force [28][29][30]) inside the soft material is also a viable option. This will allow the detection of other modalities.

As part of our research toward safer social robots for children with autism [31][32][33], this experimental setup was developed to investigate safety in social robots by considering a scenario where a small robot is thrown to the child's head [34][35][36][37][38][39]. Hence, a head mass of 3 kg was selected to make the developed dummy head comparable to that of children's dummy heads [40]. Both head parts were augmented with clay to reach this mass (Fig. 3). The masses of the parts were measured using a weight scale (Fig. 4). If the goal is to study an adult's head, then a higher dummy head mass should be considered (e.g. 4.5 kg).

A tri-axial accelerometer (ADXL 377, SparkFun Electronics, USA) was embedded inside the clay at the center of the front part of the dummy head (Fig. 5). This accelerometer will be used to measure the linear acceleration of the dummy head. The ribbon cable of the accelerometer was routed out of the head through the opening at the bottom (Fig. 6). Pressure was applied to merge the two parts of the head together. The plastic elbows were attached to the head with the Velcro straps (Fig. 6). The straps should provide more pressure to keep the head intact. Next, the dummy head was placed inside the experimental frame with the nylon coated ropes (Fig. 7). The ropes should be arranged so that the head is at the center of the experimental setup.

Figure 2: The 3D printed head parts after applying the soft material.
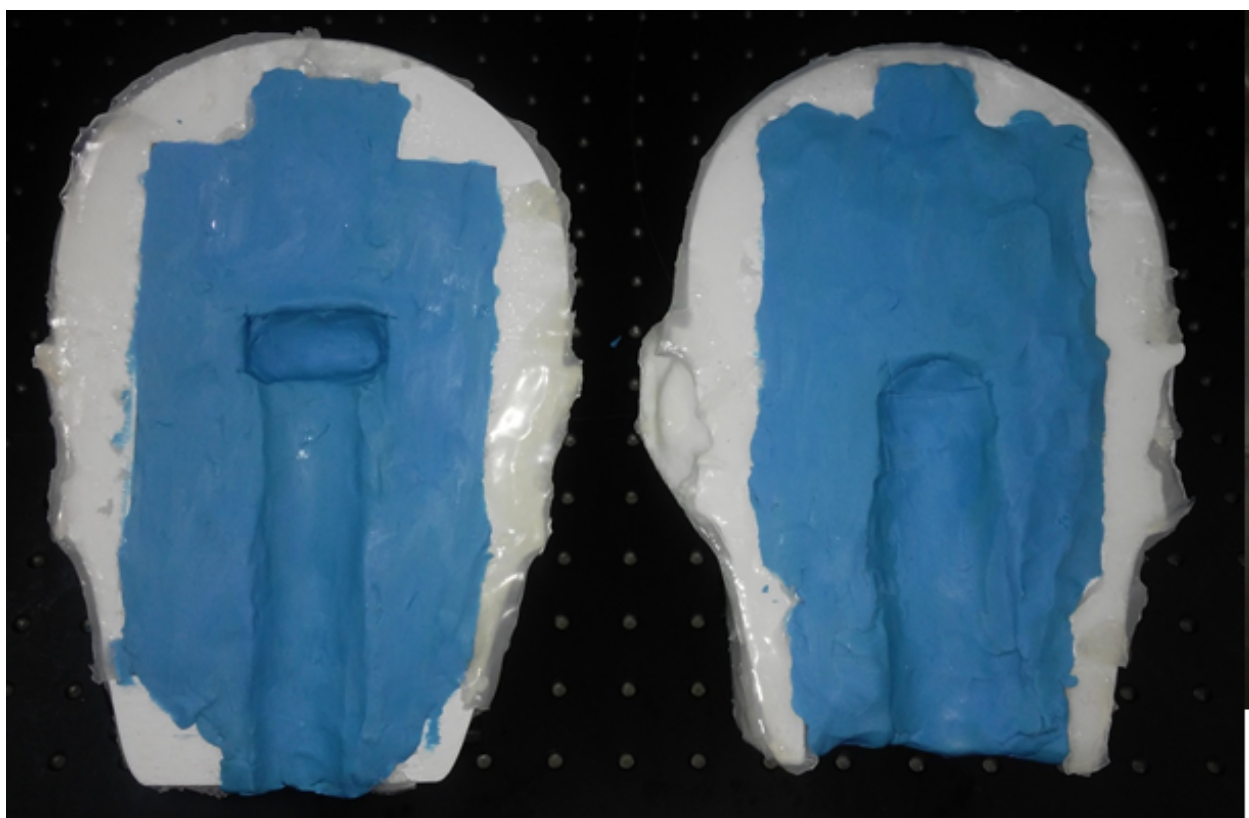

Figure 3: The 3D printed head parts after adding the clay to reach the desirable mass.

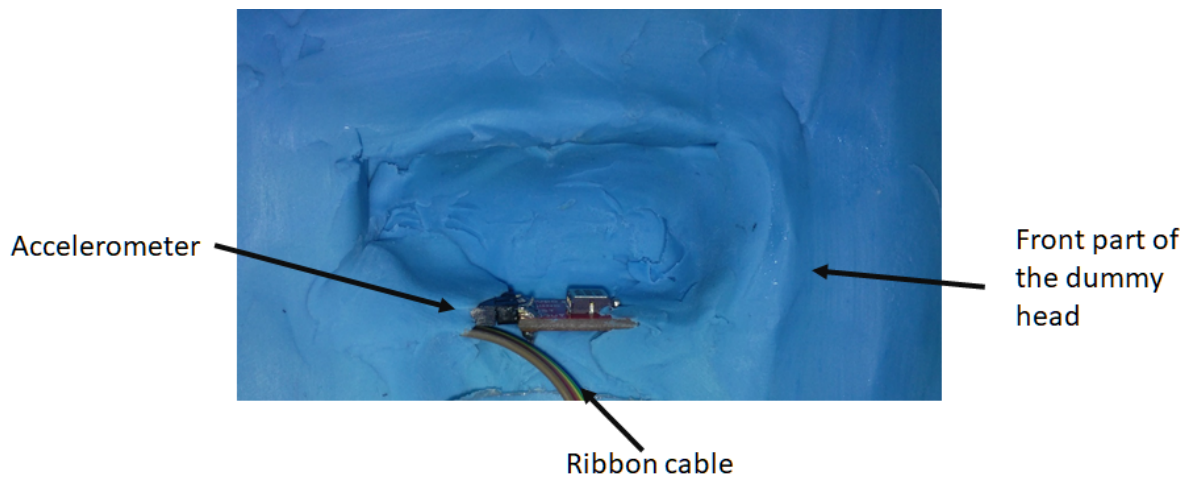Figure 4: The measured mass of the dummy head parts.

Figure 5: The accelerometer placed inside the dummy head.

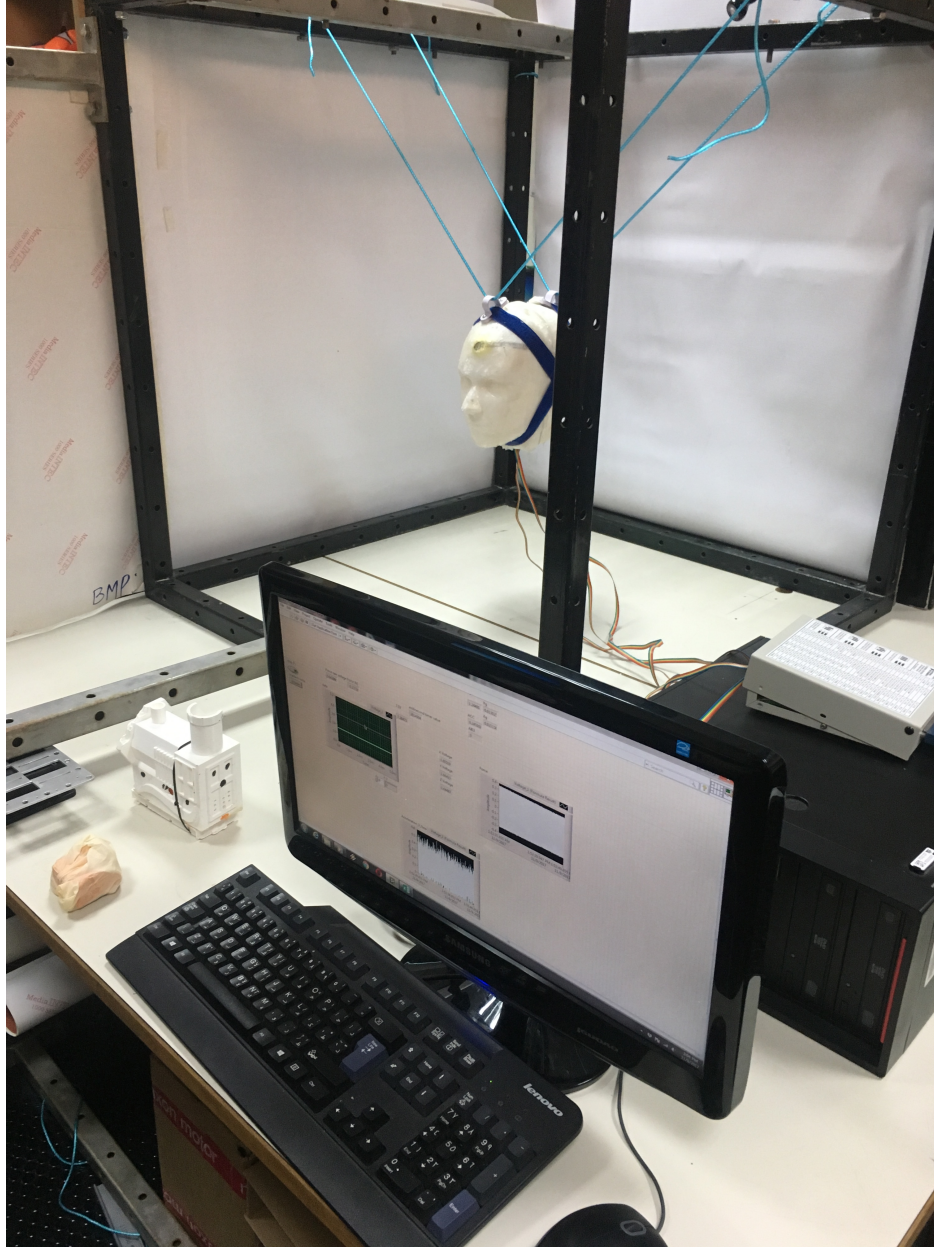Figure 6: The dummy head after assembling it with the Velcro straps.

Figure 7: Complete overview of the experimental setup. With kind permission from Springer Science + Business Media, adapted from [34].
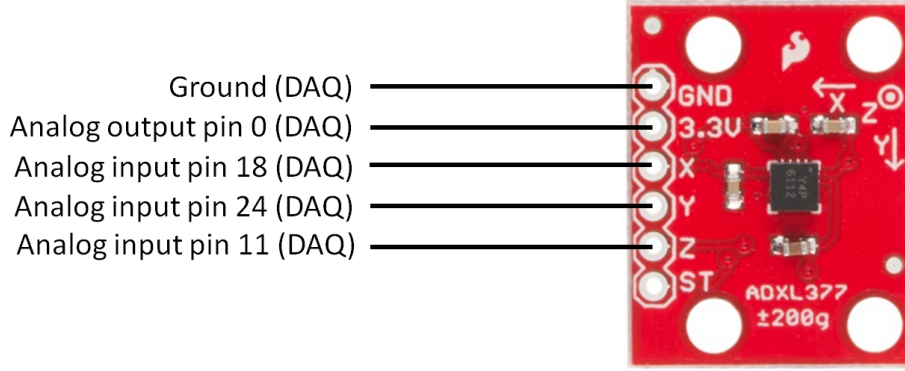
Figure 8: The mapping of the accelerometer pins to the data acquisition card (DAQ). The analog output pin 0 of the DAQ was used to provide 3.3 V to power up the accelerometer. Alternatively, an external power supply can be used.

6.2 Sensor calibration

The accelerometer was interfaced to a computer through a data acquisition card (DAQ). The ribbon cable of the accelerometer was connected to the appropriate pins of the DAQ (Fig. 8). These pins were matched with the configuration of the LabView script (Fig. (9)). Different configurations and pins can be considered depending on the DAQ model being used. A microcontroller-based DAQ that is capable of acquiring the data at a high rate can also be considered [27]. The LabView script read the voltages of the DAQ pins that were connected to the X, Y, and Z pins of the accelerometer at a sampling rate of 20 kHz and then filtered according to Channel Frequency Class 60 [41]. The readings were then converted to acceleration values (g) for each axis based on the following relation:

$$A_{axis} = \frac{|V_{current} - V_{zero}|}{Sensitivity_{axis}} \tag{2}$$

where $V_{current}$ is the current reading of the voltage of an axis (e.g. X, Y, and Z), V_{zero} is the voltage value of that axis at 0 g, and the sensitivity of an axis is the amount of voltage change that corresponds to gravitational change of one unit (g). The typical sensitivity of the accelerometer is around 6.5 mV/g based on the datasheet. More accurate sensitivity can be obtained experimentally by finding the voltage difference at 1 g and 0 g for each axis. The 0 g voltage was found by setting the axis studied parallel to ground surface while 1 g voltage by setting the axis perpendicular to the ground surface, for example, making the top surface of the accelerometer facing upward will give 1 g at the z axis while rotating it 90° will give 0 g. The sensitivity for each axis can be obtained accordingly. The sensitivity and V_{zero} values for each axis should be updated in the LabView script (i.e. labview_script.ni) by updating the formula vi (Fig. 10).

The magnitude of the resultant acceleration is based on the square root of the sum of the squares of the individual accelerations. The relation is represented as follows:

$$|A| = \sqrt{A_x^2 + A_y^2 + A_z^2} \tag{3}$$

where A_x is the magnitude of acceleration in the X direction, A_y is the magnitude of acceleration in the Y direction, and A_z is the magnitude of acceleration in the Z direction.
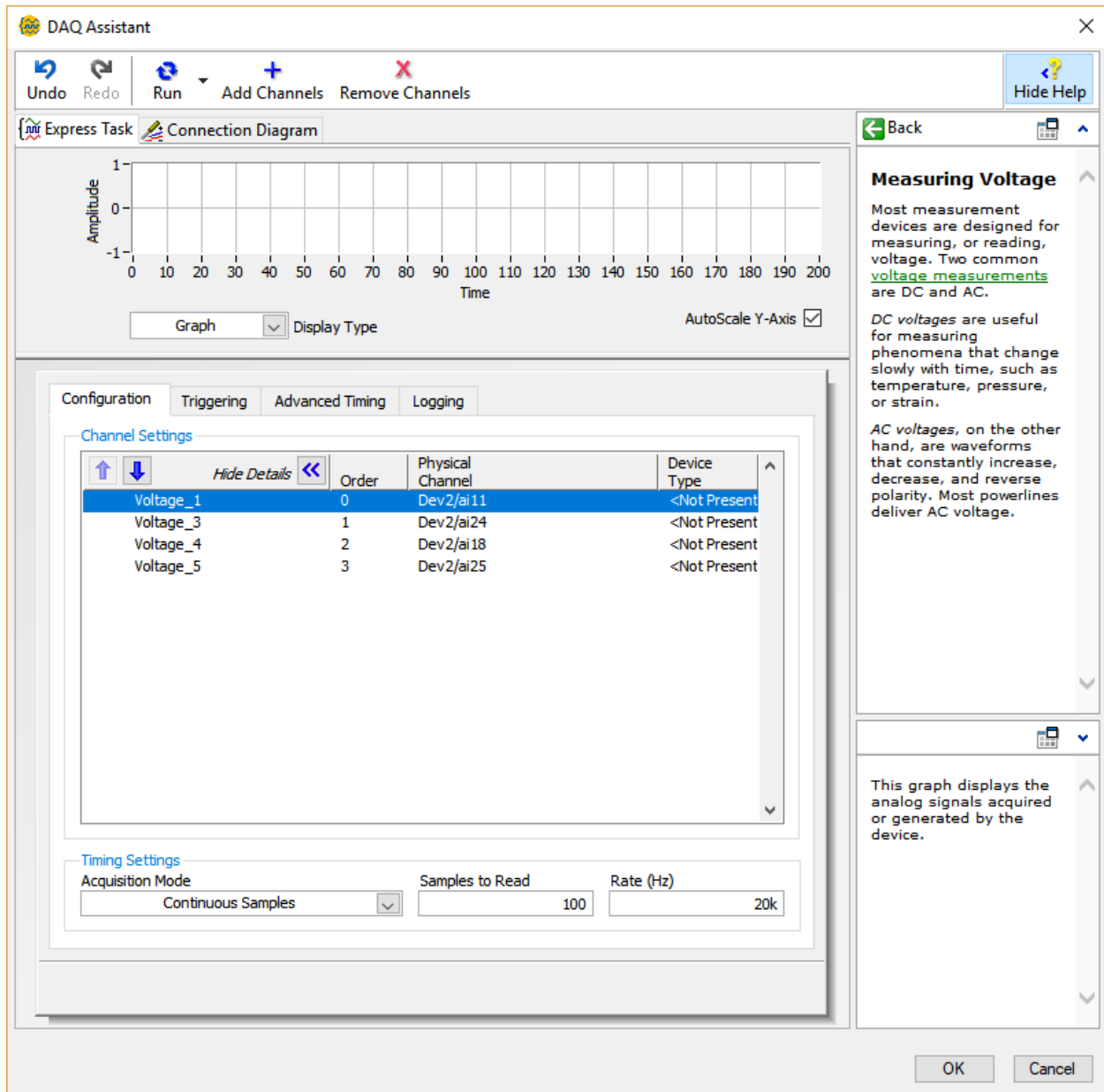
Figure 9: The analog input pins configuration of the data acquisition card (DAQ) within the LabView script. Reading the analog input pin 25 is optional and it was used for testing purposes.
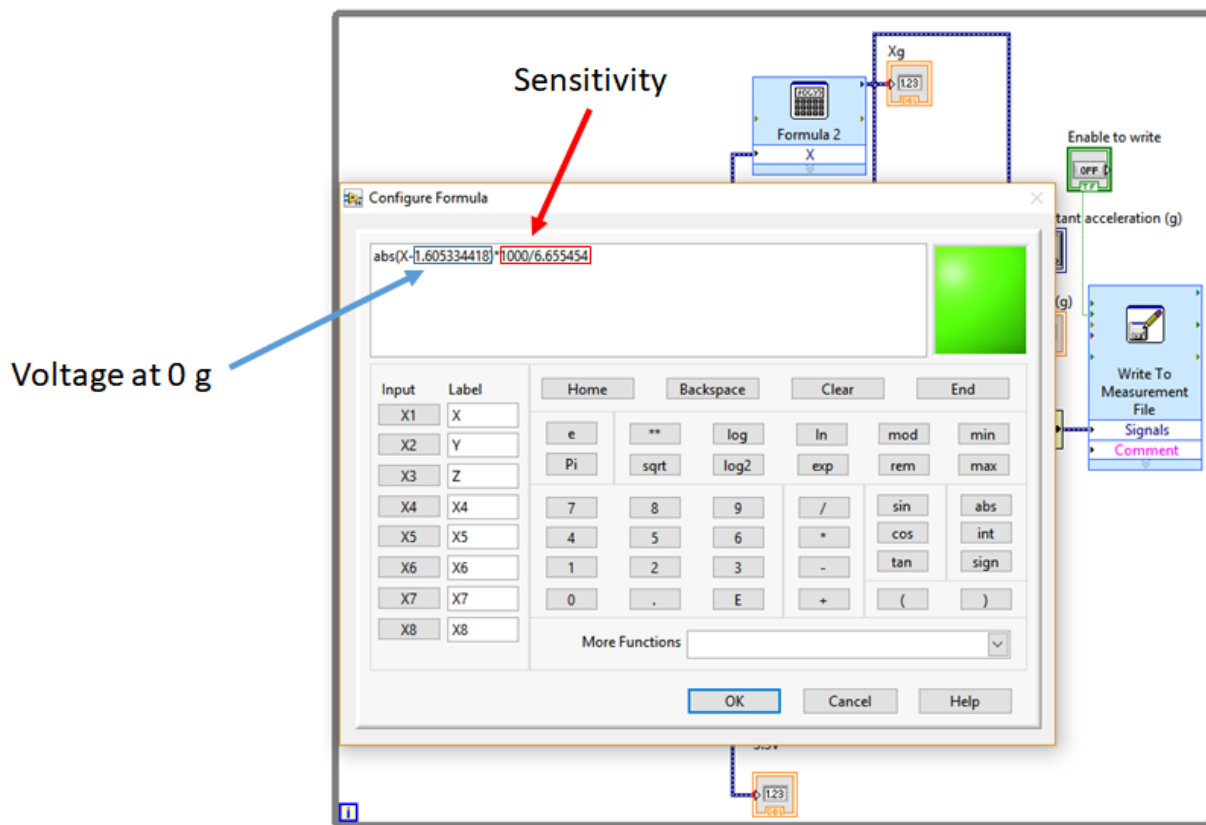
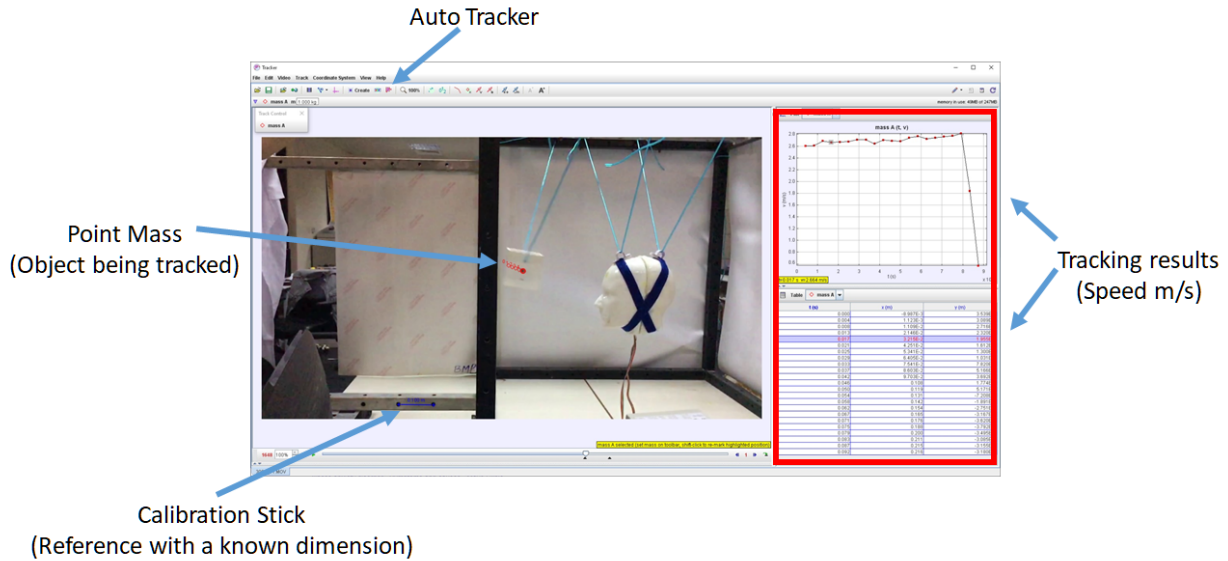Figure 10: Updating the formula vi for the X-axis.

Figure 11: A video of an impact test being analyzed for the velocity of impact in the video analysis software.

7. Operation instructions

7.1 Preparation of the test rig

There are some steps that need to done before conducting any impact experiment. The steps are as follows:

- Check the connections of the DAQ and the accelerometer and their functionality. This can be achieved by running the LabView script and performing a test experiment (e.g. light nudge to the head) and checking the response.

- Ensure that there is a fixed reference (e.g. ruler) with a known dimension that is placed along the direction of impacts and perpendicular to the head (Fig. 11). An ideal location would be under the head. This reference will be used to scale the dimensions in the video analysis software to determine the impact velocity.

- Set up the camera on the tripod in such way so that it faces the experimental setup from the side. The center view of the camera should be as centered and close to the head (Fig. 11). The reference rod and the impactor should be visible.

7.2 Conducting an experiment

Two experimenters are recommended to conduct an experiment. One is in charge of performing the impact tests while the other is in charge of recording the videos. The operations involved are as follows:

1. Load the LabView script (i.e. labview_script.ni) and configure the *Write to Measurement File* to specify the folder and the appropriate file name (Fig. 12).
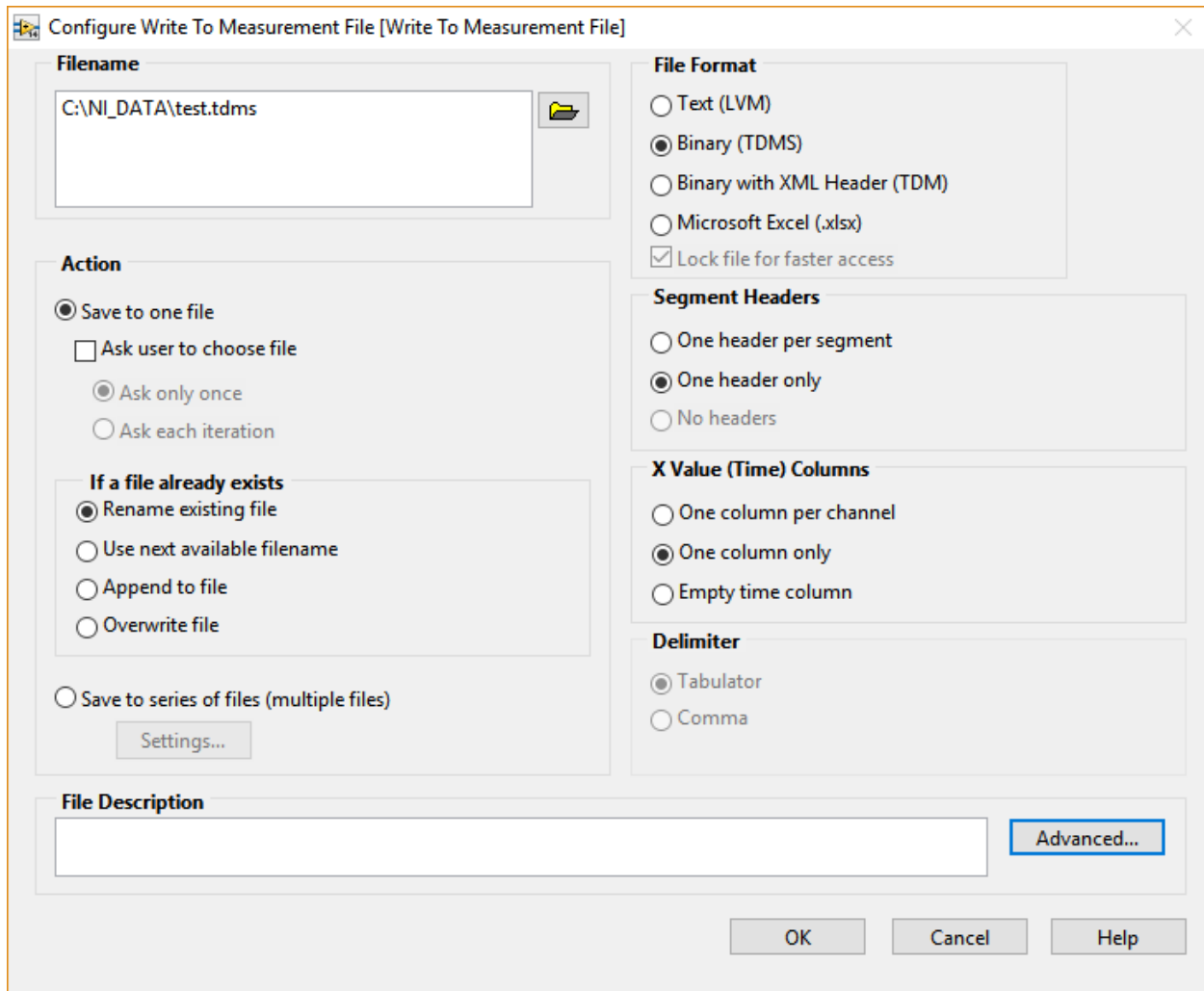
Figure 12: Specifying a folder and file name in the LabView script to store the acquired data.

2. Run the script and click *Enable to write* to start acquiring the acceleration data. Concurrently, start the video recording.

3. While conducting an experiment, the experimenter, who is releasing the impactor, should be aligned to the center of the setup and targeting the front side of the dummy head.

4. After conducting an experiment, the *Enable to write* should be clicked again to stop writing to the file. The script and the video recording should be stopped.

5. Repeat the same steps for multiple experiments.

The LabView script saves the data in Technical Data Management Streaming (TDMS) file format. Hence, an Add-In package need to be installed to be able to read the file in Microsoft Excel [42].

7.3 Video analysis

The video recordings of experiments were analyzed to obtain the impact velocities. An open-source video analysis software (Version 5.0.7, Douglas Brown, Open Source Physics) was used[4]. The steps involved in analyzing a video are as follows:

1. Run the software and load the video file. Move the *start frame* arrow to the start of the experiment and the *end frame* arrow after the impactor hits the dummy head. It is best to mark the start of an experiment after the impactor passes through the frame.

2. Add the *Calibration Stick* and mark both ends to the reference measurement (Fig. 11).

3. Create *Point Mass* by clicking *Create* in the menu bar. This will be used to track the object in the next step.

4. Click *Auto Tracker* icon to open the menu for autotracking. Press *Shift + Ctrl* and click on a feature on the impactor to select a feature to track.

5. After selecting a feature to track on the current frame, press *Search* to allow the software to automatically track the feature in the next frames of the video. Manual intervention might be needed to correctly track the feature in the next frame.

6. To view the velocity plot, change the Y-axis on the plot to *v: velocity magnitude*.

7.4 Data analysis

The data analysis involves calculating the three severity indices from the acceleration data. A MATLAB script (i.e. Matlab_script_multi.m) was used to find the Head Acceleration Criterion (HIC), 3 ms criterion, and peak head acceleration (Fig. 13). It can process multiple files and store the results in a spreadsheet file. The steps involved to analyze the data are as follows:

1. An excel file (i.e. xlsx) should be created for each experiment that contains the time and the resultant acceleration columns of the TDMS files from the experiments.

2. Each excel file should be named *trial_%d.xlsx* where *%d* is the experiment number (e.g. 1, 2, etc) placed with the script in the same folder.

3. The script is set to read 9 files. However, line 5 in the MATLAB script can be changed to match the number of files that are needed to be analyzed.

4. After running the script, the code creates a file *processed_new.xlsx* that contains the results of the analysis (Fig. 14).

8. Validation and characterization

8.1 Severity indices

The experimental setup is capable of reporting three severity indices, namely, the Head Acceleration Criterion (HIC), 3 ms criterion, and peak head acceleration. To validate the accuracy of the impact rig in reporting comparable severity indices values, impact experiments at different velocities were

---

[4]Visit the software website for more details about the options and settings of the software [43].
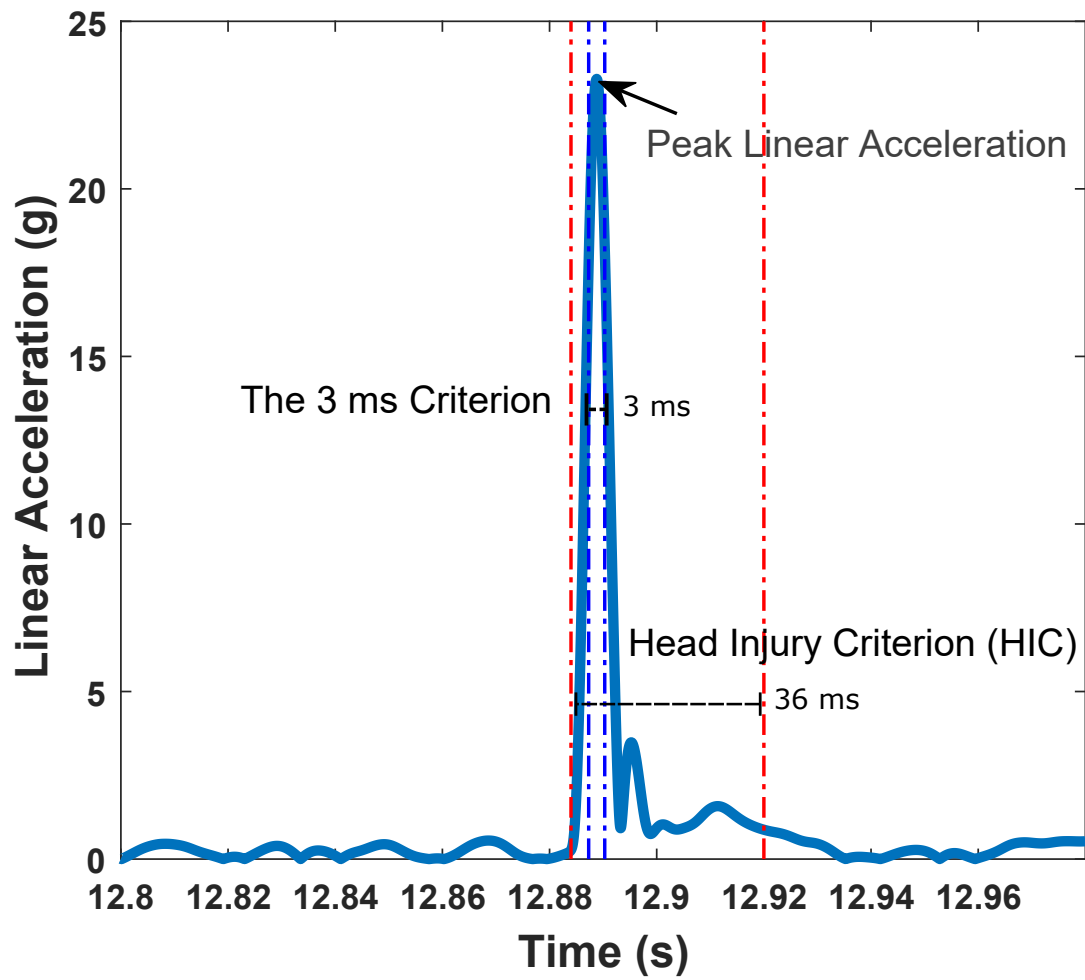
Figure 13: A sample of the generated linear acceleration data demonstrating the analysis for the three severity indices. With kind permission from Springer Science + Business Media, adapted from [34].

Figure 14: A sample of a generated analysis for 9 experiments.

performed. In these impacts, a beam with a 2 kg mass attached at one end was used as an impactor (Fig. 15). The impactor was attached to the experimental setup to allow it to hit the frontal side of the dummy head (see supplementary material). Impact tests at different velocities were conducted. The data of the experiments and video recordings were analyzed for the severity indices and impact velocities, respectively.

The results were used to evaluate the test rig by comparing the results to previous studies [5][7]. In these studies, an impactor with a mass of 1 kg was attached to different robotic arms of different masses that were then used to perform impact tests on a developed dummy head. Their setup was able to produce comparable results when compared to that produced by an anthropomorphic test dummy (ATD). The validation impacts of our experimental setup was able to produce comparable results (Fig. 16 and Fig. 17). The differences in the masses of the dummy heads and impactors are the reasons for slight differences in the results [44][45].

8.2 Limitations

This test rig is a suitable platform to evaluate the level of harm due to impacts, especially when considered for small objects (i.e. less than 3 kg) thrown at low velocities (i.e. less than 10 m/s). Furthermore, it can be used to investigate a relationship between the severity indices employed in the setup and some of the parameters (e.g. mass) of impactors. The artificial skin could also be used as an indicator for tissue injuries. However, re-applying the soft material might be needed in case of a tear or damage. Heavy impactors with sharp features should be avoided as it might penetrate the 3D printed structure of the dummy head.

9. Declaration of interest

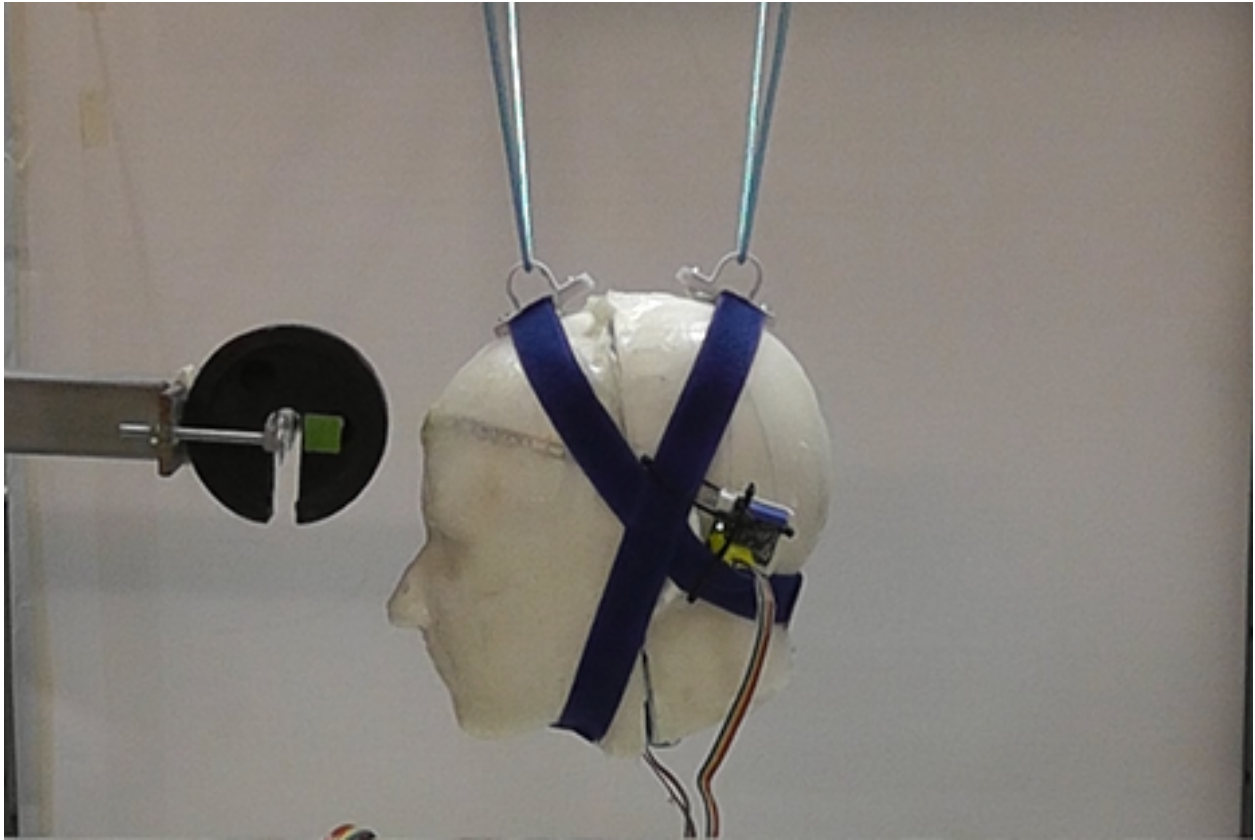The authors declare that they have no conflict of interest.

Figure 15: A sample of the validation impact tests. With kind permission from Springer Science + Business Media, adapted from [34].
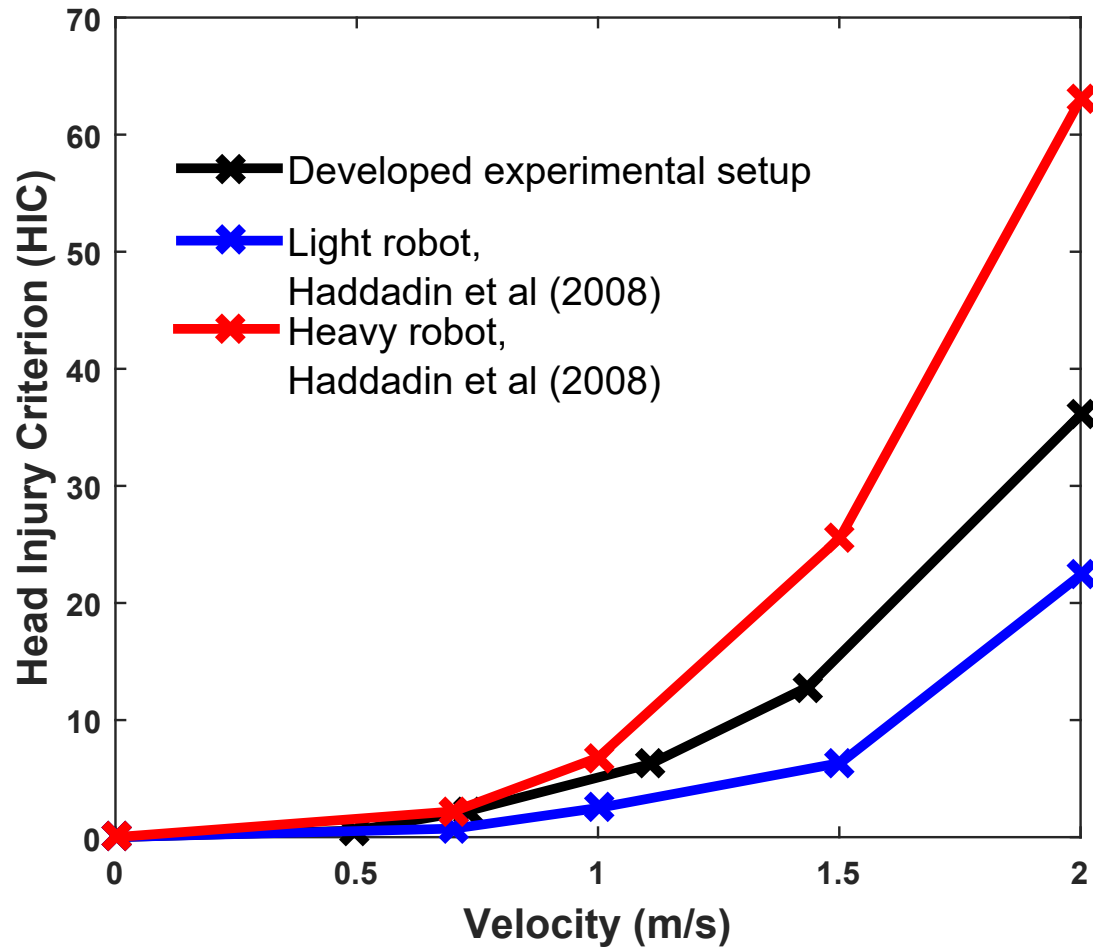
Figure 16: The Head injury criterion (HIC) results for the validation experiments. With kind permission from Springer Science + Business Media, adapted from [34].
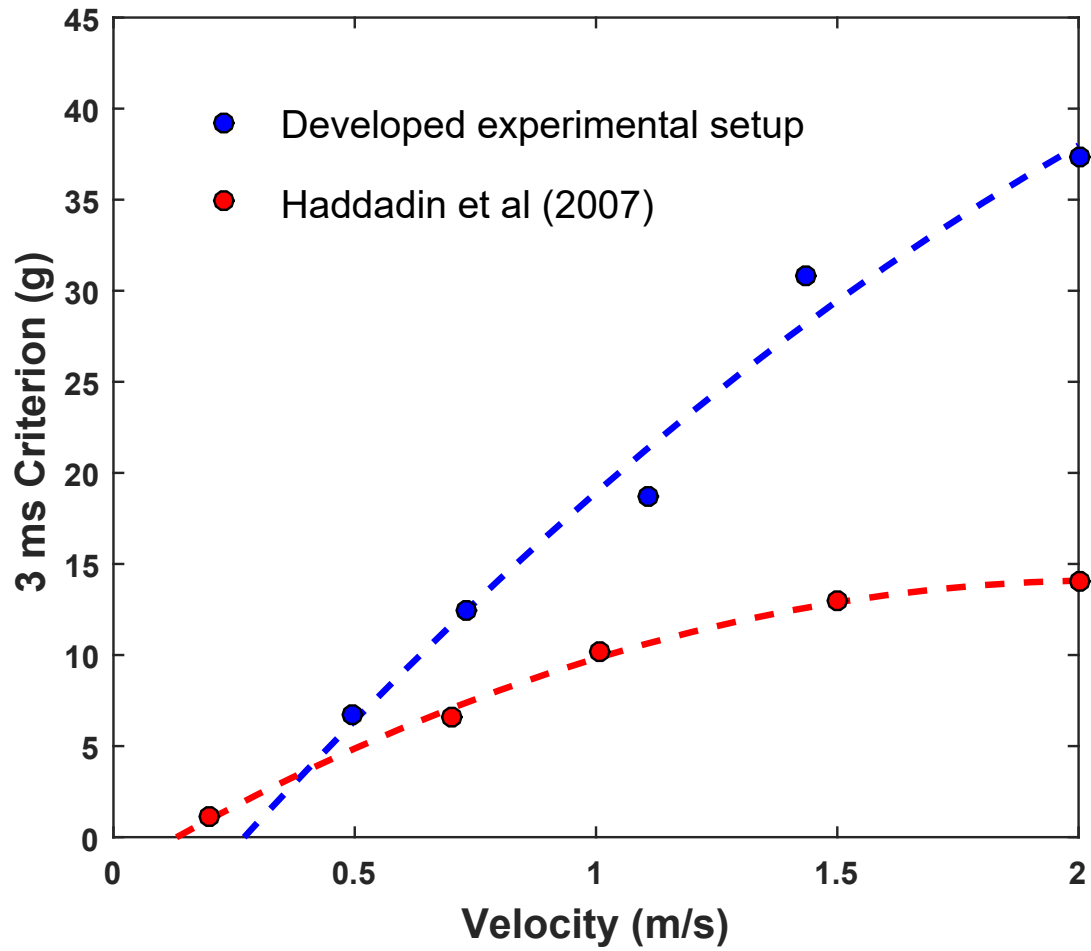
Figure 17: The 3 ms results for the validation experiments. With kind permission from Springer Science + Business Media, adapted from [34].

10. Acknowledgments

References

[1] L. Greenspan, B. A. Mclellan, H. Greig, Abbreviated injury scale and injury severity score: a scoring chart., Journal of Trauma and Acute Care Surgery 25 (1) (1985) 60–64.

[2] N. H. Yang, K. A. Rodowicz, D. Dainty, Baseball Head Impacts to the Non-Helmeted and Helmeted Hydrid III ATD, in: ASME 2014 International Mechanical Engineering Congress and Exposition, American Society of Mechanical Engineers, 2014, pp. V003T03A007–V003T03A007.

[3] A. S. McIntosh, D. Janda, Evaluation of cricket helmet performance and comparison with baseball and ice hockey helmets, British journal of sports medicine 37 (4) (2003) 325–330.

[4] G. P. Fife, D. M. O'sullivan, W. Pieter, D. P. Cook, T. W. Kaminski, Effects of olympic-style taekwondo kicks on an instrumented head-form and resultant injury measures, Br J Sports Med (2012) bjsports–2012.

[5] S. Haddadin, A. Albu-Schäffer, G. Hirzinger, Safety evaluation of physical human-robot interaction via crash-testing., in: Robotics: Science and Systems, Vol. 3, 2007, pp. 217–224.

[6] S. Haddadin, A. Albu-Schäffer, G. Hirzinger, Requirements for safe robots: Measurements, analysis and new insights, The International Journal of Robotics Research 28 (11-12) (2009) 1507–1527.

[7] S. Haddadin, A. Albu-Schaffer, G. Hirzinger, The role of the robot mass and velocity in physical human-robot interaction-part i: Non-constrained blunt impacts, in: Robotics and Automation, 2008. ICRA 2008. IEEE International Conference on, IEEE, 2008, pp. 1331–1338.

[8] H. T. Teo, J.-J. Cabibihan, Toward soft, robust robots for children with autism spectrum disorder., in: FinE-R@ IROS, 2015, pp. 15–19.

[9] C. A. Cordero, G. Carbone, M. Ceccarelli, J. Echávarri, J. L. Muñoz, Experimental tests in human–robot collision evaluation and characterization of a new safety index for robot operation, Mechanism and machine theory 80 (2014) 184–199.

[10] J. Versace, A review of the severity index, Tech. rep., SAE Technical Paper (1971).

[11] N. Euro, Assessment protocol-child occupant protection (2016).

[12] R. M. Greenwald, J. T. Gwin, J. J. Chu, J. J. Crisco, Head impact severity measures for evaluating mild traumatic brain injury risk exposure, Neurosurgery 62 (4) (2008) 789–798.

[13] S. Rowson, S. M. Duma, Brain injury prediction: assessing the combined probability of concussion using linear and rotational head acceleration, Annals of biomedical engineering 41 (5) (2013) 873–882.

[14] T. J. Young, R. W. Daniel, S. Rowson, S. M. Duma, Head impact exposure in youth football: elementary school ages 7-8 years and the effect of returning players, Clinical journal of sport medicine 24 (5) (2014) 416–421.

[15] L. L. Bakhos, G. R. Lockhart, R. Myers, J. G. Linakis, Emergency department visits for concussion in young child athletes, Pediatrics 126 (3) (2010) e550–e556.

[16] L. Zhang, K. H. Yang, A. I. King, A proposed injury threshold for mild traumatic brain injury, Transactions-American Society of Mechanical Engineers Journal of Biomechanical Engineering 126 (2) (2004) 226–236.

[17] J. P. Mihalik, J. T. Blackburn, R. M. Greenwald, R. C. Cantu, S. W. Marshall, K. M. Guskiewicz, Collision type and player anticipation affect head impact severity among youth ice hockey players, Pediatrics 125 (6) (2010) e1394–e1401.

[18] L. Zhang, K. H. Yang, A. I. King, Comparison of brain responses between frontal and lateral impacts by finite element modeling, Journal of neurotrauma 18 (1) (2001) 21–30.

[19] O. A. Shergold, N. A. Fleck, Experimental investigation into the deep penetration of soft solids by sharp and blunt punches, with application to the piercing of skin, Journal of biomechanical engineering 127 (5) (2005) 838–848.

[20] C. Sussman, B. M. Bates-Jensen, Wound care: a collaborative practice manual, Lippincott Williams & Wilkins, 2007.

[21] J.-J. Cabibihan, M. K. Abubasha, N. Thakor, A method for 3-d printing patient-specific prosthetic arms with high accuracy shape and size, IEEE Access 6 (2018) 25029–25039.

[22] J.-J. Cabibihan, S. S. Chauhan, S. Suresh, Effects of the artificial skin's thickness on the subsurface pressure profiles of flat, curved, and braille surfaces, IEEE Sensors Journal 14 (7) (2014) 2118–2128.

[23] J.-J. Cabibihan, R. Pradipta, Y. Z. Chew, S. S. Ge, Towards humanlike social touch for prosthetics and sociable robotics: Handshake experiments and finger phalange indentations, in: FIRA RoboWorld Congress, Springer, 2009, pp. 73–79.

[24] J.-J. Cabibihan, M. C. Carrozza, P. Dario, S. Pattofatto, M. Jomaa, A. Benallal, The uncanny valley and the search for human skin-like materials for a prosthetic fingertip, in: 2006 6th IEEE-RAS International Conference on Humanoid Robots, IEEE, 2006, pp. 474–477.

[25] J.-J. Cabibihan, S. Pattofatto, M. Jomâa, A. Benallal, M. C. Carrozza, P. Dario, The conformance test for robotic/prosthetic fingertip skins, in: The First IEEE/RAS-EMBS International Conference on Biomedical Robotics and Biomechatronics, 2006. BioRob 2006., IEEE, 2006, pp. 561–566.

[26] J.-J. Cabibihan, D. Joshi, Y. M. Srinivasa, M. A. Chan, A. Muruganantham, Illusory sense of human touch from a warm and soft artificial hand, IEEE Transactions on Neural Systems and Rehabilitation Engineering 23 (3) (2015) 517–527.

[27] A. R. Husain, Y. Hadad, M. N. H. Z. Alam, Development of low-cost microcontroller-based interface for data acquisition and control of microbioreactor operation, Journal of Laboratory Automation 21 (5) (2016) 660–670.

[28] J.-J. Cabibihan, K. K. Sadasivuni, A. Y. Alhaddad, Biometric liveness detection through biocompatible capacitive sensor, US Patent App. 16/058,453 (Feb. 14 2019).

[29] K. Sadasivuni, A. Al Haddad, H. Javed, W. Yoon, J.-J. Cabibihan, Strain, pressure, temperature, proximity, and tactile sensors from biopolymer composites, in: Biopolymer Composites in Electronics, Elsevier, 2017, pp. 437–457.

[30] A. Y. Alhaddad, S. E. AlKhatib, R. A. Khan, S. M. Ismail, A.-S. S. Shehadeh, A. M. Sadeq, J.-J. Cabibihan, Toward 3D printed prosthetic hands that can satisfy psychosocial needs: Grasping force comparisons between a prosthetic hand and human hands, in: A. Kheddar, E. Yoshida, S. S. Ge, K. Suzuki, J.-J. Cabibihan, F. Eyssel, H. He (Eds.), Social Robotics, Springer International Publishing, Cham, 2017, pp. 304–313.

[31] A. Y. Alhaddad, H. Javed, O. Connor, B. Banire, D. Al Thani, J.-J. Cabibihan, Robotic trains as an educational and therapeutic tool for autism spectrum disorder intervention, in: W. Lepuschitz, M. Merdan, G. Koppensteiner, R. Balogh, D. Obdržálek (Eds.), Robotics in Education, Springer International Publishing, Cham, 2019, pp. 249–262.

[32] J. Cabibihan, H. Javed, K. Sadasivuni, A. Al Haddad, Smart robotic therapeutic learning toy, WIPO Patent WO2018033857, World Intellectual Property Organization.

[33] J.-J. Cabibihan, R. Chellali, C. W. C. So, M. Aldosari, O. Connor, A. Y. Alhaddad, H. Javed, Social robots and wearable sensors for mitigating meltdowns in autism - A pilot test, in: S. S. Ge, J.-J. Cabibihan, M. A. Salichs, E. Broadbent, H. He, A. R. Wagner, Á. Castro-González (Eds.), Social Robotics, Springer International Publishing, Cham, 2018, pp. 103–114.

[34] A. Y. Alhaddad, J.-J. Cabibihan, A. Bonarini, Head impact severity measures for small social robots thrown during meltdown in autism, International Journal of Social Robotics 11 (2) (2018) 255–270. `doi:10.1007/s12369-018-0494-3`.

[35] A. Y. Alhaddad, J.-J. Cabibihan, A. Hayek, A. Bonarini, Safety experiments for small robots investigating the potential of soft materials in mitigating the harm to the head due to impacts, SN Applied Sciences 1 (5). `doi:10.1007/s42452-019-0467-7`.

[36] A. Y. Alhaddad, J.-J. Cabibihan, A. Hayek, A. Bonarini, Data on the impact of objects with different shapes, masses, and impact velocities on a dummy head, Data in brief 22 (2019) 344–348.

[37] A. Y. Alhaddad, J.-J. Cabibihan, A. Hayek, A. Bonarini, Data on the impact of an object with different thicknesses of different soft materials at different impact velocities on a dummy head, Data in Brief 24 (2019) 103885. `doi:10.1016/j.dib.2019.103885`.

[38] A. Y. Alhaddad, J.-J. Cabibihan, A. Hayek, A. Bonarini, The impact of different shaped objects of different masses at different impact velocities on a dummy head (dataset) (2018). `doi:10.7910/DVN/AVC8GG`.

[39] A. Y. Alhaddad, J.-J. Cabibihan, A. Hayek, A. Bonarini, The impact of an object with different thicknesses of different soft materials at different impact velocities on a dummy head (dataset) (2019). `doi:10.7910/DVN/TXOPUH`.

[40] Solutions, Humanetics Innovative, Hybrid iii 3 year old child(Date last accessed 22-Mar-2019). URL `http://www.humaneticsatd.com/crash-test-dummies/children/hiii-3yo`

[41] Society of Automotive Engineers, Instrumentation for impact test—part 1—electronic instrumentation, SAE 211, (1995).

[42] National Instruments, Tdm excel add-in for microsoft excel download, (Date last accessed 22-Mar-2019).
URL http://www.ni.com/example/27944/en/

[43] D. Brown, Tracker 5.0.7, (Date last accessed 22-Mar-2019).
URL https://physlets.org/tracker/

[44] T. P. Hutchinson, Peak acceleration during impact with helmet materials: effects of impactor mass and speed, European journal of sport science 14 (sup1) (2014) S377–S382.

[45] R. Martin, L. Liptai, S. Yerby, K. Williams, The relationship between mass and acceleration for impacts on padded surfaces, Journal of biomechanics 27 (3) (1994) 361–364.